

A novel Flip-OFDM optical communication system based on lazy lifting wavelet transform for intensity modulated direct detection

SİNEM TEMURTAŞ^{1,*}, GAMZE TOPRAKCI², ALİ ÖZEN¹

¹Tarsus University, Department of Electrical and Electronics Engineering, 33400 Tarsus, Turkey

²Türk Telekom, Kalpaklıoğlu Road, No:4, Hunat, 38030 Kayseri, Turkey

In this article, a novel optical OFDM (LLWT Flip-OFDM) waveform based on Lazy Lifting wavelet transform (LLWT) is recommended to enhance the success of Flip-OFDM communication system, which is one of the optical OFDM methods used in visible light communication systems. In the proposed scheme, superior advantages of LWT transform such as ICI and ISI suppression capabilities because of its good time-frequency localization properties and orthonormal structure are utilized, unlike fast Fourier transform (FFT). In order to confirm the success of the proposed waveform through the bit error rate (BER) achievement benchmark, computer simulation studies are executed in the indoor multipath optical channel and underwater multipath optical channel environment. It is perceived from the acquired results that with the suggested LLWT Flip-OFDM communication scheme, 7.5 dB SNR gain is achieved against the Flip-OFDM communication system and 22.5 dB SNR improvement is performed versus the VLC-OFDM communication system.

(Received November 10, 2021; accepted February 6, 2023)

Keywords: Visible light communications, Optical OFDM, Flip-OFDM, Lifting wavelet transform, LLWT Flip-OFDM, VLC-OFDM

1. Introduction

The increasing request for wide band implementations has led to a massive increase in cellular data traffic. To satisfy the greatly increased request for high band-width services, networks must be updated to encourage higher information speeds. Copper-based schemes that have come the saturation point in capacity and access cannot provide high capacities with bulk sending remoteness. Fiber or photonic schemes have appeared as a natural alternative to copper-based schemes to perform extreme broad bandwidth sending media.

Visible light optical communication, like for example infrared (IR) [1] and ultraviolet (UV) [2], is a shape of telecommunications that utilizes light to transport knowledge. This shape of optical wireless communication (OWC) has enormous potential for high-rate data communication because of the availability of approximately 670 THz of unlicensed spectrum. In visible light communications (VLC), signals utilize the visible light spectrum from 375 nm to 750 nm, which is approximately 10,000 times greater than the Radio Frequency (RF) bandwidth. VLC utilizes Light emitting diodes (LED) as transmitter and photo diodes as receiver. Operating in the visible light spectrum, LED performs the double aim of lighting and communication, making VLC the preferred selection in indoor wireless communication schemes. VLC has been the focus of interest in the last decade because of its energy savings and spectrum relaxation in wireless communication compared to RF communication systems.

Communication utilizing visible light is not a novel

idea. The earliest shape of visible light communication can be followed back to a time when people utilized fire signals and smoke signals to transmit information over greater distances. The first recorded utilization of visible light in communication can be attributed to Alexander Graham Bell for his photophone in 1880 [3]. He managed an experiment to illustrate the transmission of voice knowledge over a distance of 200 meters over sunlight. Fluorescent light is also utilized for low data speed transmission [4]. Investigation on VLC began at Keio University, Japan with the aim of developing, planning and standardizing VLC systems [5]. In 2003, the visible light communications consortium (VLCC) was founded to standardize VLC technologies [5]. There are several research organizations and groups working on VLC, like for example the Japan electronics and information technology industries associations (JEITA), home gigabit access (OMEGA) [6], and the task group. In 2001 Twibright Labs improved RONJA (Reasonable Optical near Joint Access) a free space optical communication network over a distance of 1.4 km [7]. The utilize of white LEDs for communication was demonstrated in 2000 by Tanaka et al. [8]. IEEE 802.15.7. VLC standardization began in 2007 as JEITA released two standards, CP-1221 and CP-1222. The first IEEE VLC standard, IEEE 802.15.7, was released in 2011 with data speed varying from 11.67 kbit/s to 96 Mbit/s, with several physical layers (PHYs) and media access control (MAC) layers [9, 10]. VLC systems; It has been developed as an alternative to wireless communication tools like for example Wi-Fi, Bluetooth, ZigBEE, RF. VLC systems have been added to the Wireless Network IEEE 802.15.7 standard under the

name of short distance optical communication, which supports multi-layer technology capable of high-speed data transfer [11]. In 2010, the OMEGA Project aimed to develop a home access optical wireless network to study with RF technology [12].

For short distance optical communications like for example device-to-device interconnects in local area networks, Intensity Modulated Direct Detection (IM/DD) schemes are accepted to complex coherent sensing based schemes to reduce whole scheme burden. In IM/DD schemes, the information speed is restricted by the bandwidth from electrical to optical and optical to electrical conversions. Therefore, as using simple on-off keying modulation on a single optical wave-length, the whole information speed is restricted to level gigabits per second. One possible approximation to maximize the information speed per wave-length is to perform modulation schemes with high spectral productivity [13].

Orthogonal Frequency Division Multiplexing (OFDM) is a type of multi-carrier modulation included into many wireless standards because of its various benefits like for example robustness versus frequency selective fading channels, easy single-tap equalization, high spectral productivity, and simple digital modulator/demodulator application. In IM/DD optical schemes, the electrical signal operating the light source must be real and positive. Conventional radio OFDM signals that are complex and bipolar cannot be employed in IM/DD schemes.

Many multi-carrier modulations (MCM)-based unipolar methods suitable for IM/DD schemes have been recommended to map the light source attribute. Unipolar OFDM can be practically applied in optical communication [14, 15] and amplitude modulated RF wireless telecommunication. In these telecommunication systems, channel distribution and multipath fading can cause inter-symbol interference and decrease system success. Unipolar OFDMs can reduce these effects and achieve better inter-symbol interference (ISI) levels. Moreover, as discussed in the research literature [16], unipolar OFDMs can be both power and spectrally efficient compared to other modulation schemes like for example PPM [17] and ON-OFF switching [17]. In the research literature, DC-biased Optical OFDM (DCO-OFDM) and Asymmetrically Clipped Optical OFDM (ACO-OFDM) are the most known. DCO-OFDM is composed of appending a DC bias to convert the true bipolar MCM data to a unipolar data, resulting in an optically power unproductive solution. In ACO-OFDM, merely single sub-carriers are modulated, resulting in an antisymmetric time-region data. The resulting bi-polar data is later made positive by clipping the whole negative sequence. ACO-OFDM has greater optical power productivity than DCO-OFDM as merely the positive section is sent. However, ACO-OFDM suffers from spectral inefficiency as merely single sub-carriers are employed to transport signal. Hybrid schemes combining the two simple methods have been recommended to enhance the spectral and power productivities of IM/DD schemes. But these schemes have complex architectures,

so raising the complexity and burden of IM/DD schemes. However, one of the most important examples of unipolar OFDM is Flip-OFDM. Flip-OFDM is an alternative technique recommended in a patent, but its achievement and full potential has not been much explored in the literature. In this study, we will first introduce the Flip-OFDM system and then present the proposed Lazy Lifting Wavelet Transform (LLWT) based Flip-OFDM scheme to improve the achievement of the Flip-OFDM scheme.

In addition to these, the wavelet transform takes advantage of unit length wavelet data produced from the multilevel tree structured wavelet family. Because of its better orthogonality and greater band productivity, discrete wavelet transform (DWT) can be utilized in fast Fourier transform (FFT) based communication systems. The wavelet transform (WT) method has higher spectral productivity and is more resistant to inter-carrier interference (ICI) [18, 19]. DWT, which has become attractive recently, is one of the robust methods for digital modulation [20, 21].

The most basic reason for using DWT in the multi-carrier communication system structure is that it is based on orthogonality. Wavelets can be planned to accomplish better frequency localization and can eliminate the need for guard intervals by overlapping symbols in the time domain. This overlapping attribute increases symbol duration and thus provides better spectral productivity. Also, the use of wavelet filters provides greater flexibility, suggests a higher degree of stopband attenuation, and results in good side lobe suppression [22].

However, filters used in DWT processes include complex mathematical processes, the Lifting wavelet transform (LWT) scheme has been improved to decrease the complexity. LWT, which has been utilized in image and signal processing implementations in recently, is employed to mitigate many deficiencies of the standard WT. Lifting wavelet transform is purposed to decrease the computational burden in WT and substitute for DWT utilized in the computation of wavelet coefficients [22]. Lifting scheme is the simplest and most productive scheme for WT [23]. When FFT and DWT are compared with LWT, LWT's; It has advantages such as reduced computational complexity, better frequency localization and power consumption compared to the filter bank structure, easy applicability on the hardware side due to significantly reduced computational complexity.

Because the Inverse LWT (ILWT) transform uses zero padding, it multiplexes the data applied to its input. This, in turn, spreads the transmitted data, reducing the impact of mistakes caused by the noise and interference influences of the channel. Also, since wavelets have an orthonormal structure, they have excellent reconstruction properties, ICI and ISI suppression capabilities.

In this article, a novel ILWT spread Flip-OFDM communication system is proposed by taking advantage of the data spreading feature of the ILWT transform. In this developed study, inspired by [24-26], it is suggested to combine Flip-OFDM method and Lazy LWT (LLWT) conversion to enhance the success of Flip-OFDM communication schemes. Thus, it is seen from the

computer simulation results that remarkable performances are obtained in BER successes in wireless communication schemes where the LLWT-Flip-OFDM scheme is applied. Even though there are evaluations in the literature [27] on the DWT-Flip-OFDM system in order to improve the performances, as far as the authors know, there has been no study examining Flip-OFDM communication systems by combining Flip-OFDM and LLWT.

High reliability is evaluated by the bit error rate (BER) and is highly significant for schemes where mistakes are less tolerable. For these reasons, BER changes were used as a comparison metric in our analyzes.

The remaining of the study is planned as following; In

Section 2, the general structure of the Flip-OFDM communication scheme is introduced briefly. In Section 3, explanations are given about the proposed LLWT-based Flip-OFDM structure. Finally, computer simulation results and evaluations are given in Sections 4 and 5.

2. Flip-OFDM optical wireless communications

The unit diagram of the Flip-OFDM OWC scheme is given in Fig. 1.

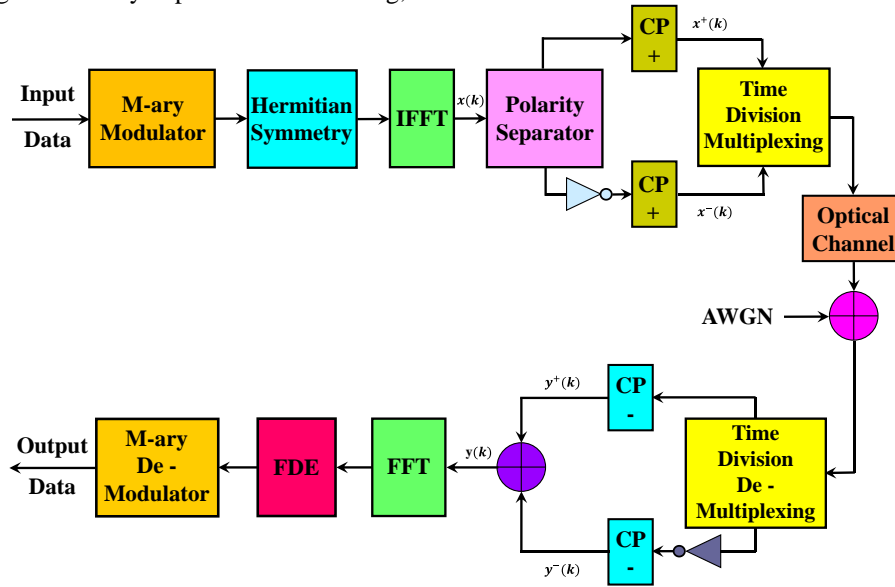


Fig. 1. Transceiver structure of Flip OFDM OWC system (color online)

Randomly generated serial input data in the sender part of the Flip-OFDM OWC model illustrated in Fig. 1 are mapped relying on the number of data to be transmitted with a carrier in the M-ary Modulator Unit. After that, the modulated data are subjected to Hermitian symmetry processing in the Hermitian Symmetry Unit to acquire real numbers at the IFFT Unit output. To create Hermitian symmetry, data vectors of $T_s = T_{sym}/N$ duration formed by the modulated signal are operated in parallel units. The modulated data in the frequency region are in the shape of $[X = X_0, X_1, \dots, X_{N-1}]^T$ and have a Hermitian symmetrical structure. This structure is provided by fixing 0 (DC) and $N/2$ sub-carriers to zero. The identical of a characteristic Hermitian symmetric form in the frequency region can be provided by the next formula:

$$X[k] = \begin{cases} 0, & \text{if } k = 0 \\ X[k], & \text{if } k = 1, 2, \dots, \left(\frac{N}{2}\right) - 1 \\ X^*[N - k], & \text{if } k = \left(\frac{N}{2}\right) + 1, \left(\frac{N}{2}\right) + 2, \dots, N \\ 0, & \text{if } k = \frac{N}{2} \end{cases} \quad (1)$$

where (*) represents the complex conjugate processes.

Later, at the IFFT Unit output, a bipolar data is

acquired in the time region as provided in the formula below.

$$x(k) = x^+(k) + x^-(k) \quad (2)$$

Here, $x^+(k)$ denotes the positive part of the signal and $x^-(k)$ the negative part. In order to acquire the unipolar data from here, the positive and negative sections of the data are separated as illustrated in the next formulas.

$$x^+(k) = \begin{cases} x(k), & x(k) \geq 0 \\ 0, & \text{other} \end{cases} \quad (3)$$

$$x^-(k) = \begin{cases} x(k), & x(k) < 0 \\ 0, & \text{other} \end{cases} \quad (4)$$

The real-time bipolar data separation is done utilizing a Polarity Separator as depicted in Fig. 1. A polarity inverter is utilized to acquire the polarity inverted data of the negative section $x^-(k)$, i.e. its absolute value is taken, $-x^-(k)$. The positive part $x^+(k)$ and the polarity reversed negative section $-x^-(k)$ are sent separately over two sequential OFDM blocks. The positive data is sent in the

first sub-block of OFDM and the polarity reversed negative data is sent in the second sub-block of OFDM. By adding a periodic prefix (CP) to each OFDM sub-block, time division multiplexing is performed in the Time Division Multiplexing Block to obtain Flip-OFDM data packages. The produced Flip-OFDM data packages are sent via the optical multi-path fading channel through LEDs and arrive the receiver after being degraded by additive white Gaussian noise (AWGN). After the corrupted data arriving the receiver are reconstructed with appropriate time domain or frequency domain equalizers, the determined data at the M-ary De-Modulator Unit output are acquired by implementing the inverse of the procedures executed on the sender part. After that desired success measures like for example BER and PAPR are computed.

3. The proposed Lazy Lifting Wavelet Transform based Flip-OFDM (LLWT-Flip-OFDM)

3.1. Basis of the discrete wavelet transform

The Wavelet Transform has recently gained a lot of popularity in the field of signal processing since it has the capability to provide both time and frequency information simultaneously, hence it gives a time-frequency representation of the signal. The DWT wavelets are transformation techniques with desirable characteristics of localization both in time and frequency. They also possess the property of orthogonality across scale and translation. The DWT provides a means of decomposing sequences of real numbers in a basis of compactly supported orthonormal sequences each of which is related by being a scaled and shifted version of a single function. A Haar wavelet is the simplest type of wavelet.

Mathematical analysis of the DWT, using Haar wavelet family, is presented below [28, 29]:

Haar wavelet is described by

$$\vartheta_{01} = \begin{cases} +1, & \text{if } 0 \leq t \leq \frac{1}{2} \\ -1, & \text{if } \frac{1}{2} \leq t \leq 1 \\ 0, & \text{where else} \end{cases} \quad (5)$$

To Haar wavelet family corresponds the reconstruction low-pass filter h_r and high-pass filter g_r are presented as following formulas:

$$h_r = \frac{\sqrt{2}}{2} [1, 1] \quad (6)$$

$$g_r = \frac{\sqrt{2}}{2} [1, -1] \quad (7)$$

For simplicity, the wavelet family reconstructor having two branches is illustrated in the next Fig. 2.

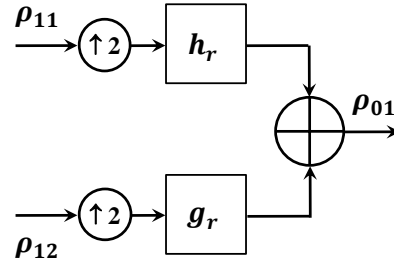


Fig. 2. Two band reconstructor

ρ_{11} and ρ_{12} are depicting the two binary signals which belong to $\{1, -1\}$. The resulting ρ_{01} sequence is defined by

$$\rho_{01}(n) = (\rho_{11}(\uparrow 2) * h_r)(n) + (\rho_{12}(\uparrow 2) * g_r)(n) \quad (8)$$

here $*$ shows convolution operator, $\rho_{11}(\uparrow 2)$ and $\rho_{12}(\uparrow 2)$ are the results of dyadic up sampling.

$$\rho_{11}(n) = \sum_{k=0}^1 h_r(k) \rho_{11}^{(\uparrow 2)}(n-k) + \sum_{k=0}^1 g_r(k) \rho_{12}^{(\uparrow 2)}(n-k) \quad (9)$$

Since h_r and g_r are two quadrature mirror filter (QMF) i.e. $h_r(k) = (-1)^k g_r(1-k)$ and h_r is symmetric ($h_r(k) = h_r(-k)$), we derive:

$$\rho_{11}(n) = \sum_{k=0}^1 h_r(k) [\rho_{11}^{(\uparrow 2)}(n-k) + (-1)^n \rho_{12}^{(\uparrow 2)}(n-k)] \quad (10)$$

It can be generalized the results for the upper bands.

3.2. Basis of the lifting wavelet transform

Filters employed in conventional DWT processes include complex mathematical processes, and the LWT scheme has been improved to reduce this. LWT is the new wavelet structure suggested by Sweldens, called “second generation wavelets” based on the Lifting Diagram [30]. LWT, which has been utilized in image and signal processing implementations in recently, is utilized to mitigate many deficiencies of the standard WT. LWT scheme is aimed to decrease the processing burden in WT and replace DWT which is employed in the computation of wavelet coefficients. Lifting scheme is the simplest and most efficient scheme for WT.

Mathematical analysis of the LWT is expressed below [24, 26]:

In the lifting wavelet transform method, the modulated signal is divided into odd and even samples. Instead of filters, Split Predict and Update processes are applied. Complex calculations are not required for these operations as in conventional methods. In Fig. 3, the Lifting wavelet transform is given in detail.

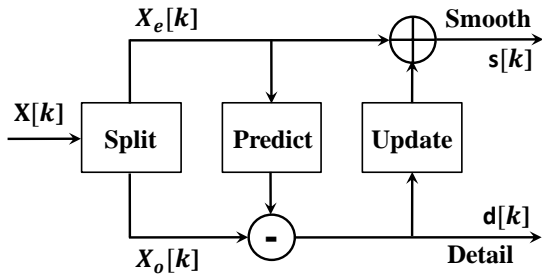


Fig. 3. Lifting wavelet transform

In the Split step, the modulated $X[k]$ signal is initially divided into odd and even components as in Equation (11) and (12).

$$X_o[k] = X[2k + 1] \quad (11)$$

$$X_e[k] = X[2k] \quad (12)$$

In the Predict part, odd samples are tried to be acquired nearly by making use of even samples. The second step, Predict, protects the high frequency components by removing the low frequency components of the modulated signal. In the prediction process, the subset $X_o[k]$ is estimated over the subset $X_e[k]$ employing the prediction operator $P(\cdot)$. The detail information of the $X[k]$ signal is acquired as in Equation (13) by taking the distinction between the subset $X_o[k]$ and the estimated $P(X_e[k])$. The $P(\cdot)$ Prediction operator is a linear combination of a single neighboring subset.

$$P(X_e[k]) = \sum_i (p_i X_e[k + i]) \quad (13)$$

where, p_i are the prediction coefficients. This step acts as a high pass filter and the high frequency components ($d[k]$) that provide the detail part of the acquired signal.

$$d[k] = X_o[k] - P(X_e[k]) \quad (14)$$

In the Update step, the samples are scaled to fix and then appended with even samples to give low pass filtered values for transformation. In the third part, update, the even components are updated by employing the detailed signal to decrease the frequency aliasing influence. In the update process, the approximate information about the signal is acquired as a result of gathering the detailed information inserting the $U(\cdot)$ Update operator with the subset $X_e[k]$. The $U(\cdot)$ Update operator is a linear combination of neighboring $d[k]$ values. The equation for the $U(\cdot)$ Update operator is stated in Equation (15).

$$U(d[k]) = \sum_i (u_i d[k + i]) \quad (15)$$

where, u_i are the updating coefficients. In the update process, the approximate value of the acquired signal by passing the signal through a low pass filter is acquired by updating the linear combination of the $d[k]$ prediction distinction as in Equation (16). These examples include low frequency components that provide approximate

information ($s[k]$) about the signal.

$$s[k] = X_e[k] + U(d[k]) \quad (16)$$

Inverse conversion is acquired by implementing the exact opposite operations employed in the transformation to the acquired $d[k]$ and $s[k]$ signals. Inverse Lifting wavelet transform is shown in Fig. 4 in detail.

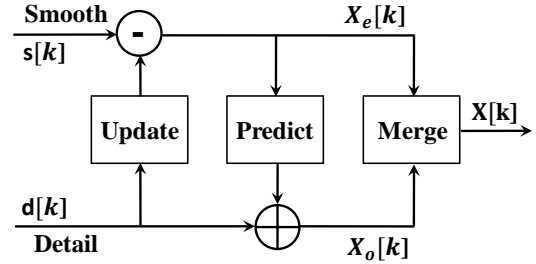


Fig. 4. Inverse Lifting wavelet transform

$$X_o[k] = d[k] + P(X_e[k]) \quad (17)$$

$$X_e[k] = s[k] - U(d[k]) \quad (18)$$

After the inverse conversion procedure, as given in Equation (19), the original modulated signal is acquired by combining the odd index and even index samples with the M combination operator.

$$X[k] = M\{X_o[k], X_e[k]\} \quad (19)$$

In addition, Prediction and Update operations are illustrated in Equation (20) with a 2×2 matrix by executing intermediate procedures. Smooth and detail information is acquired from this matrix.

$$\begin{bmatrix} d[k] \\ s[k] \end{bmatrix} = \begin{bmatrix} 1 & -P(\cdot) \\ U(\cdot) & 1 - P(\cdot)U(\cdot) \end{bmatrix} \begin{bmatrix} X_o[k] \\ X_e[k] \end{bmatrix} \quad (20)$$

$$A = \begin{bmatrix} 1 & -P(\cdot) \\ U(\cdot) & 1 - P(\cdot)U(\cdot) \end{bmatrix} \quad (21)$$

Since the determinant of the matrix shown by Equation (21) is equal to one, this matrix is an invertible matrix. Since it is the inverse of the matrix, a completely symmetric analysis can be made. The inverse-LWT shown in Fig. 4 and given by Equations (17) and (18) is mathematically expressed by equation (22) with a 2×2 matrix. The matrix in Equation (22) is the inverse of the matrix in Equation (20) (shown in equation (23)).

$$\begin{bmatrix} X_o[k] \\ X_e[k] \end{bmatrix} = \begin{bmatrix} 1 - P(\cdot)U(\cdot) & P(\cdot) \\ -U(\cdot) & 1 \end{bmatrix} \begin{bmatrix} d[k] \\ s[k] \end{bmatrix} \quad (22)$$

$$AA^{-1} = \begin{bmatrix} 1 - P(\cdot)U(\cdot) & P(\cdot) \\ -U(\cdot) & 1 \end{bmatrix} \quad (23)$$

To reconstruct the signal, it is adequate to reverse the procedures in Fig. 3 and change the signs as illustrated in Fig. 4 in ILWT block.

3.3. The proposed optical OFDM design

In this developed study, inspired by [24-26], the unit scheme of the proposed LLWT-Flip-OFDM system, which combines Flip-OFDM communication systems and LWT conversion, is shown in Fig. 5 [31].

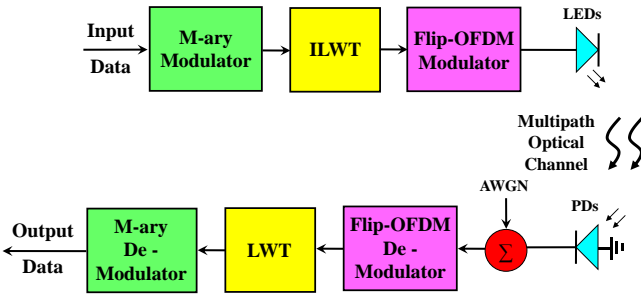


Fig. 5. The proposed LLWT-Flip-OFDM OWC system transceiver structure [31] (color online)

On the sender part of the LLWT-Flip-OFDM scheme illustrated in Fig. 5, ILWT transformation is applied to the modulated signal with the assist of the following formula (for detailed information on ILWT/LWT, please see to [24-26]).

$$V_{ILWT}[k] = \sum_{n=0}^{N-1} \sum_{z=0}^{U-1} X^n[z] 2^{\frac{n}{2}} \varphi[2^n k - z] \quad (24)$$

Here, $X^n[k]$ depicts the modulated signal, k the number of sub-carriers, $\varphi[k]$ denotes the mother wavelets with scaling factor n and shift z for each subcarrier.

Later, the spread signal at the ILWT Unit output, as explained in detail in the prior chapter, are applied to the Flip-OFDM Modulator Block, and the suggested LLWT-Flip-OFDM data packets are obtained. After the obtained data packages are sent through the multipath optical channel via LEDs and distorted with AWGN, arrive the receiver via photo diodes (PD). After the appropriate equalization processes are applied to the corrupted incoming data to the receiving side, the reverse of the processes on the transmitting side is performed. LWT conversion is applied to the resolved data at the Flip-OFDM De-Modulator Unit output with the assist of the following formula.

$$Y_{LWT}^z[k] = \sum_{n=0}^{N-1} R[n] 2^{\frac{k}{2}} \varphi[2^k n - z], \quad k = 0, 1, 2, \dots, N-1, \quad z = 0, 1, 2, \dots, N-1 \quad (25)$$

Here, $R[n]$ denotes the resolved Flip-OFDM signal.

After the acquired data at the LWT Unit output are demodulated in the M-ary De-Modulator Unit, the requested performance benchmark is calculated.

4. Numerical results and discussions

Numerical outcomes are acquired from optical channel measurements in two different environments. The first of these is done in the indoor optical channel environment, and the second is done in the underwater optical channel environment. All numerical results are produced using 64 subcarriers, 16 bit CP and 128 point FFT.

4.1. Numerical results of indoor optical channel environment

At this stage of the study, performance analyzes are made over the 5-taps indoor multipath optical channel impulse response from Reference [32]. The 5-taps multipath OCIR is given in Table 1.

Table 1. Five taps indoor multipath OCIR values [32].

Tap No	5 Taps OCIR
0	4.825E-5
1	6.030E-5
2	7.068E-5
3	7.673E-5
4	7.714E-5

Fig. 6 shows the obtained BER performances for different wavelet families of the suggested LLWT Flip-OFDM scheme over the AWGN channel for BPSK modulated signals.

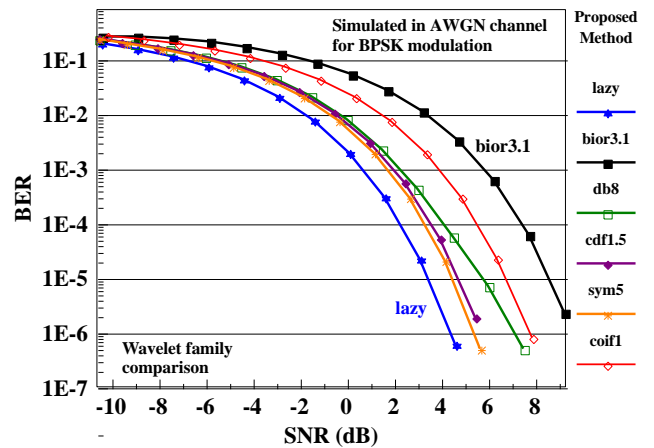


Fig. 6. Wavelet family comparison of the recommended scheme in AWGN channel for BPSK modulated signal (color online)

From the given results in Fig. 6, it is perceived that the best accomplishment is achieved with lazy wavelet. Therefore, the acquired results with the lazy wavelet are used in the next comparisons.

The performances of the proposed LLWT Flip-OFDM, Flip-OFDM and VLC-OFDM communication schemes are compared in Fig. 7 in the AWGN channel surroundings.

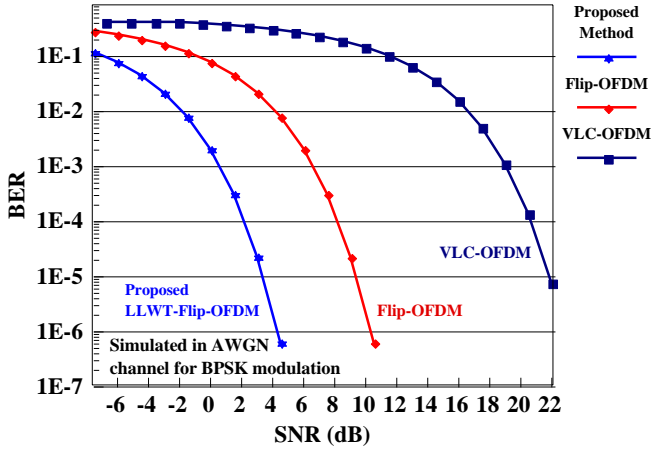


Fig. 7. Comparison of the proposed LLWT Flip-OFDM, VLC-OFDM and Flip-OFDM communication systems in AWGN channel for BPSK modulated signal (color online)

It can be observed from Fig. 7 that the proposed LLWT Flip-OFDM method provides an SNR superiority of approximately 6 dB to the Flip-OFDM system and approximately 20 dB to the VLC-OFDM system at the 1E-3 BER level.

For BPSK modulated signals, the BER performances of the proposed LLWT Flip-OFDM, Flip-OFDM and VLC-OFDM communication techniques over a single tap optical LOS flat fading channel are shown in Fig. 8. Optical LOS flat fading channel is produced utilizing only one of the multipath OCIR values given in Table 1.

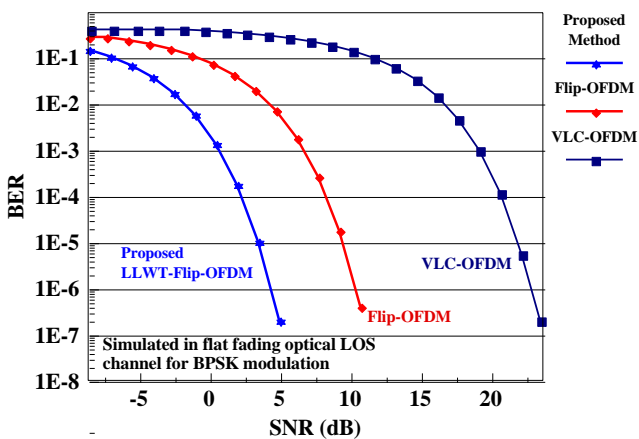


Fig. 8. Comparison of the proposed LLWT Flip-OFDM, VLC-OFDM and Flip-OFDM communication systems in flat fading optical LOS channel for BPSK modulated signal (color online)

As Fig. 8 is evaluated, it is understood that outcomes very close to AWGN channel performances are obtained. The reason for this can be clarified by the fact that the transmitter and receiver are very close to each other and

see each other directly.

The obtained BER performances for different wavelet families of the proposed LLWT Flip-OFDM method over the five-taps OCIR are shown in Fig. 9.

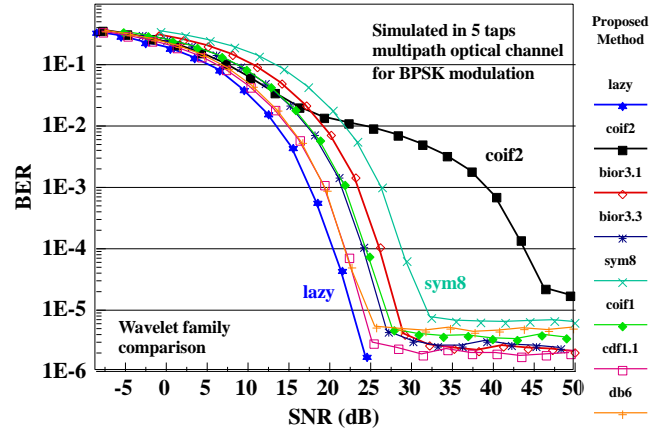


Fig. 9. Wavelet family comparison of the proposed scheme in five taps indoor OCIR for BPSK modulated signal (color online)

It is understood from the given outcomes in Fig. 9 that the best success with the proposed method is obtained with lazy wavelet. Therefore, the obtained results with the lazy wavelet are used in the next comparisons.

For BPSK modulated signals, the performances of the proposed LLWT Flip-OFDM, Flip-OFDM and VLC-OFDM communication schemes in a five-taps indoor OCIR environment are compared in Fig. 10.

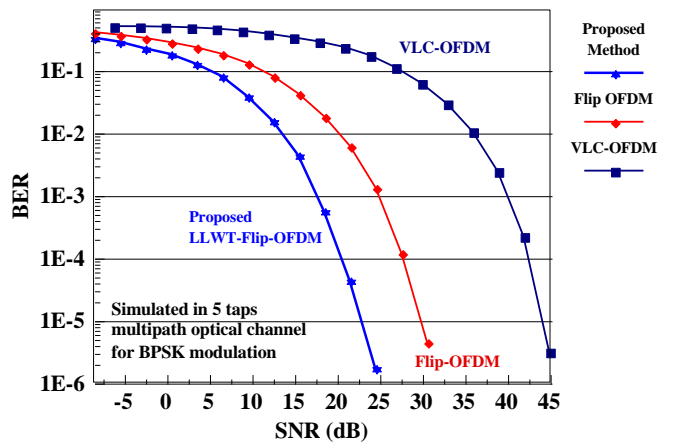


Fig. 10. Comparison of the proposed LLWT Flip-OFDM, VLC-OFDM and Flip-OFDM communication systems in five taps indoor OCIR for BPSK modulated signal (color online)

Fig. 10 shows that the proposed LLWT Flip-OFDM method provides approximately 7.5 dB SNR superiority to Flip-OFDM system and approximately 22.5 dB SNR superiority to VLC-OFDM system in an indoor OCIR environment with five taps for 1E-3 BER level.

Fig. 11 shows the obtained BER performances for different wavelet families of the proposed LLWT Flip-

OFDM method over the AWGN channel for 4-QAM modulated signals.

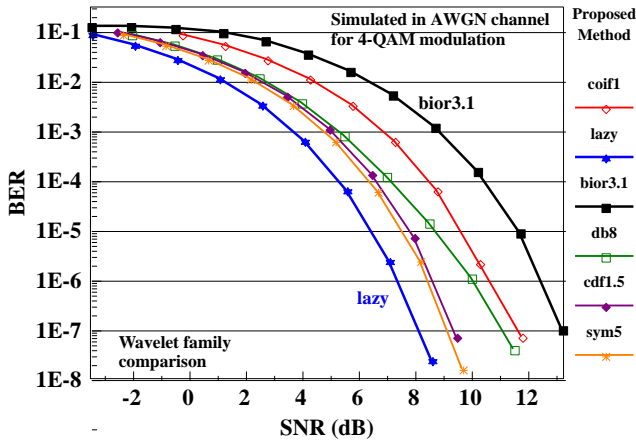


Fig. 11. Wavelet family comparison of the proposed technique in AWGN channel for 4-QAM modulated signal (color online)

From the given results in Fig. 11, it is determined that the best accomplishment is achieved with lazy wavelet. Therefore, the acquired results with the lazy wavelet are used in subsequent comparisons.

The performances of the proposed LLWT Flip-OFDM, VLC-OFDM and Flip-OFDM communication systems are evaluated in the AWGN channel environment in Fig. 12 for 4-QAM modulated signals.

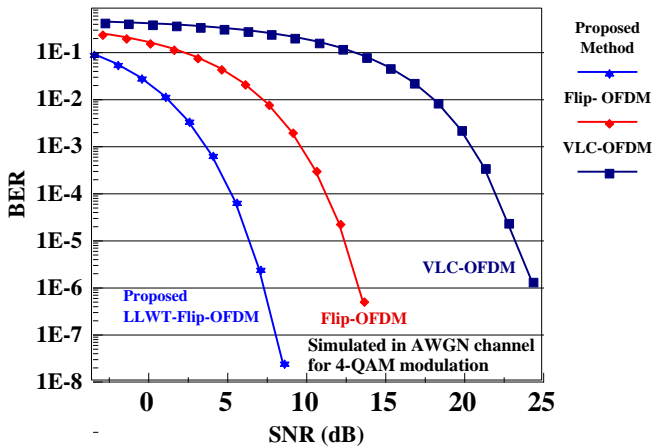


Fig. 12. Comparison of the proposed LLWT Flip-OFDM, Flip-OFDM and VLC-OFDM communication systems in AWGN channel for 4-QAM modulated signal (color online)

For 4-QAM modulated signals, it is observed from Fig. 12 that the proposed LLWT Flip-OFDM method provides an SNR superiority of approximately 6 dB to the Flip-OFDM system and approximately 17 dB to the VLC-OFDM system at the 10^{-3} BER level.

For 4-QAM modulated signals, the BER successes of the suggested LLWT Flip-OFDM, Flip-OFDM and VLC-OFDM communication techniques over a single tap optical LOS flat fading channel are shown in Fig. 13.

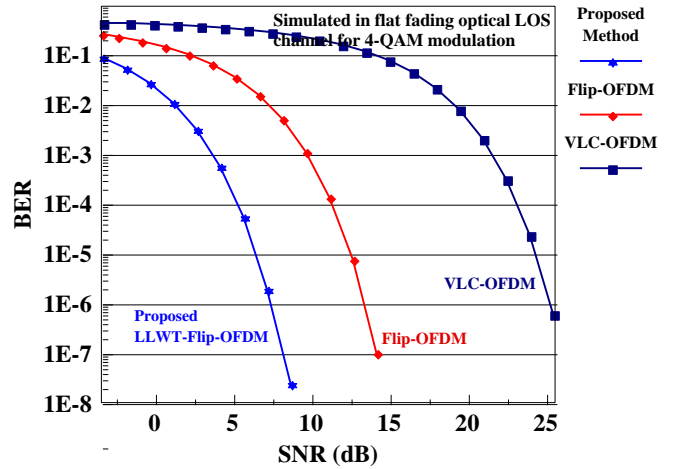


Fig. 13. Comparison of the proposed LLWT Flip-OFDM, VLC-OFDM and Flip-OFDM communication systems in flat fading optical LOS channel for 4-QAM modulated signal (color online)

As Fig. 13 is investigated, it is determined that outcomes and developments similar to AWGN channel performances are obtained.

The obtained BER performances for different wavelet families of the proposed LLWT Flip-OFDM method over a five-taps indoor OCIR for 4-QAM modulated signals are shown in Fig. 14.

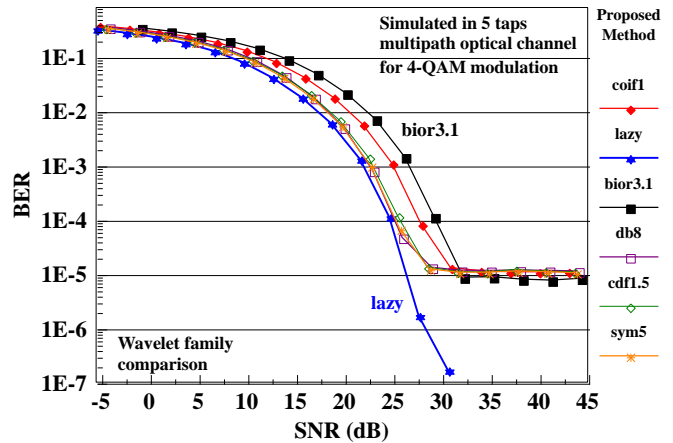


Fig. 14. Wavelet family comparison of the proposed scheme in five taps indoor OCIR for 4-QAM modulated signal (color online)

It is understood from the given outcomes in Fig. 14 that the best success with the proposed LLWT Flip-OFDM method is obtained with lazy wavelet. Therefore, the obtained results with the lazy wavelet are used in the next comparison.

For 4-QAM modulated signals, the performances of the proposed LLWT Flip-OFDM, Flip-OFDM and VLC-OFDM communication schemes are compared in a five-taps indoor OCIR environment in Fig. 15.

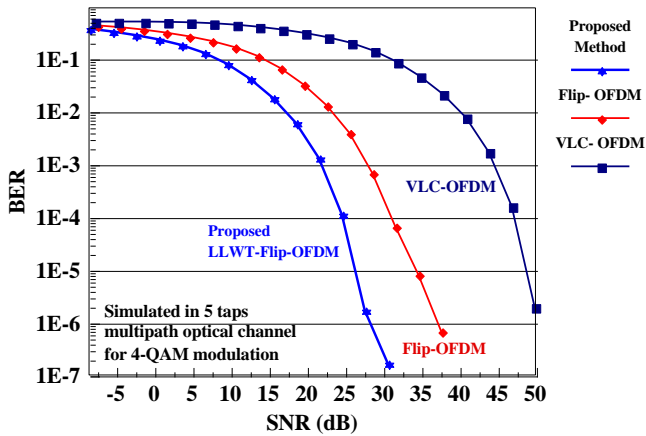


Fig. 15. Comparison of the proposed LLWT Flip-OFDM, VLC-OFDM and Flip-OFDM communication systems in five taps indoor OCIR for 4-QAM modulated signal (color online)

For 4-QAM modulated signals, it is noticed from Fig. 15 that the proposed LLWT Flip-OFDM method provides an SNR superiority of approximately 6 dB to the Flip-OFDM system and approximately 22 dB to the VLC-OFDM system in a five-branch indoor OCIR environment at the 1E-3 BER level.

4.2. Numerical results of underwater optical channel environment

In this phase of the study, performance analyzes are carried out in the underwater multipath optical channel impulse response environment with 2 taps and 3 taps taken from Reference [33]. 2-taps and 3-taps OCIR are given in Table 2.

Table 2. Two taps and three taps underwater multipath OCIR values [33]

Tap No	2 Taps OCIR	3 Taps OCIR
0	3.963E-6	2.426E-6
1	0.426E-6	0.516E-6
2		0.123E-6

In Fig. 16, the obtained BER performances for different wavelet families of the proposed LLWT Flip-OFDM method over 2-taps underwater OCIR for BPSK modulated signals are presented.

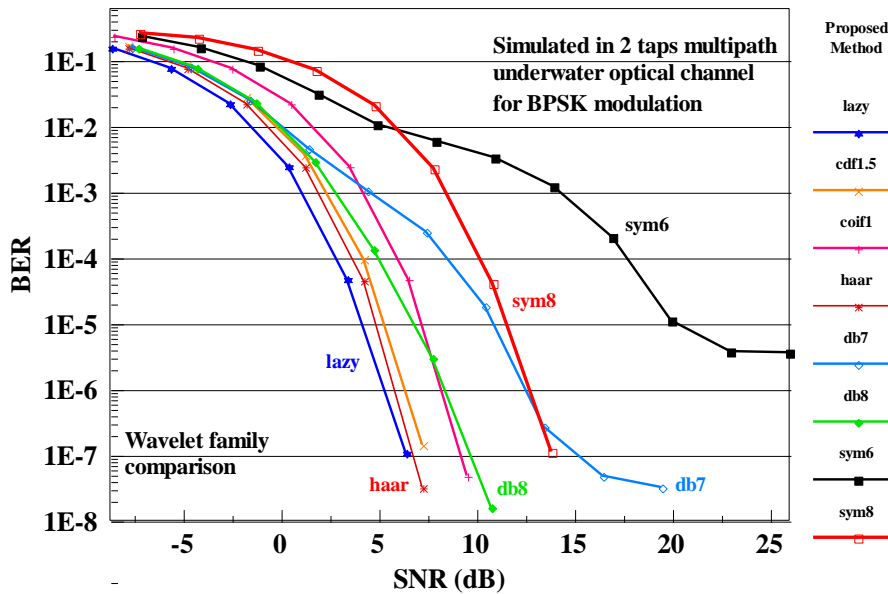


Fig. 16. Wavelet family comparison of the proposed scheme in two taps underwater OCIR for BPSK modulated signal (color online)

From the given results in Fig. 16, it is inferred that the best success is achieved with lazy wavelet. Therefore, the acquired results with the lazy wavelet are used in the next comparison.

The performances of the proposed LLWT Flip-OFDM, VLC-OFDM and Flip-OFDM communication systems are examined for BPSK modulated signals in two-taps underwater OCIR environment in Fig. 17.

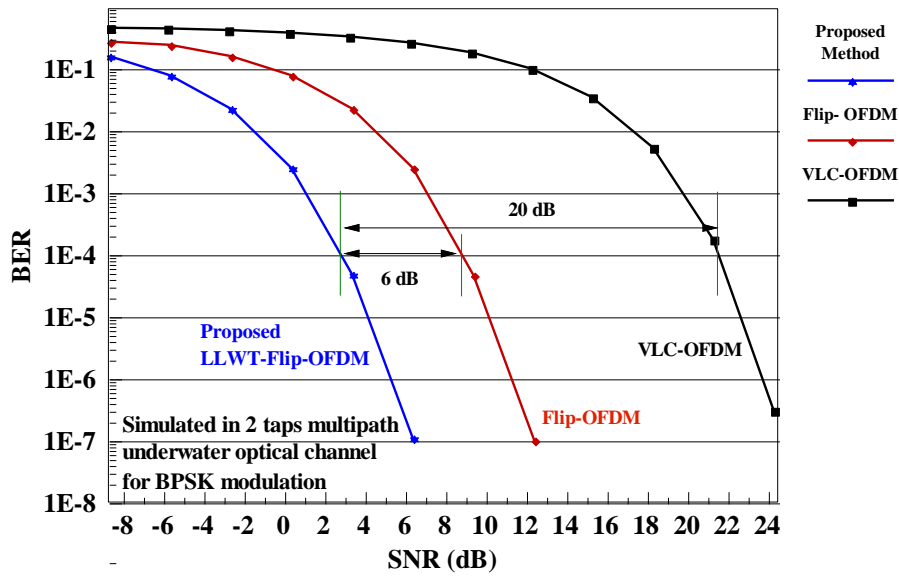


Fig. 17. Comparison of the proposed LLWT Flip-OFDM, VLC-OFDM and Flip-OFDM communication systems in two taps underwater OCIR for BPSK modulated signal (color online)

It is confirmed from Fig. 17 that the proposed LLWT Flip-OFDM method provides an SNR superiority of approximately 6 dB to the Flip-OFDM system and approximately 20 dB to the VLC-OFDM system at the $1E-3$ BER level for BPSK modulated signals.

The obtained BER performances for different wavelet families of the proposed LLWT Flip-OFDM method over 3-taps underwater OCIR for BPSK modulated signals are presented in Fig. 18.

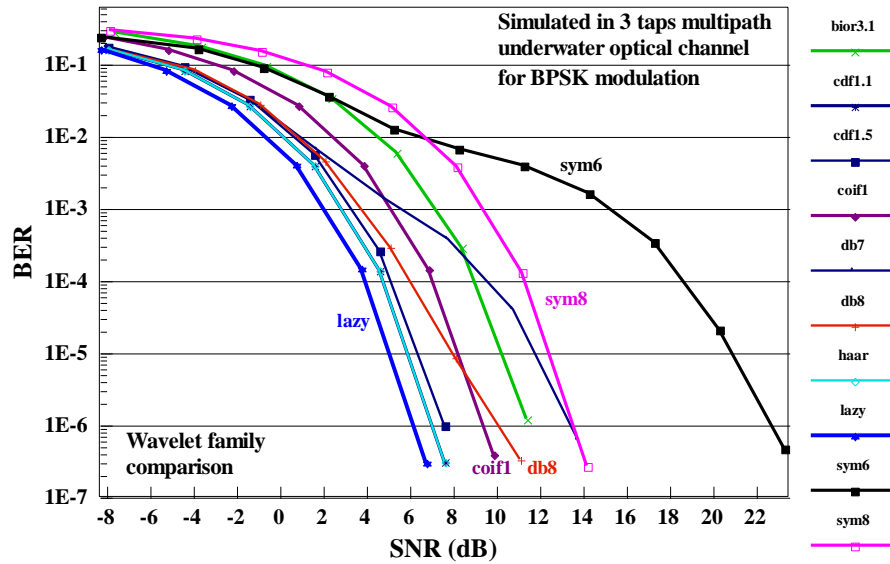


Fig. 18. Wavelet family comparison of the proposed scheme in three taps underwater OCIR for BPSK modulated signal (color online)

Similar to the two-taps underwater OCIR results, it is deduced that the best success is provided by the lazy wavelet. Therefore, the acquired results with the lazy wavelet are used in the next comparison.

The performances of the proposed LLWT Flip-OFDM, Flip-OFDM and VLC-OFDM communication systems are analyzed in a three-taps underwater OCIR environment for BPSK modulated signals in Fig. 19.

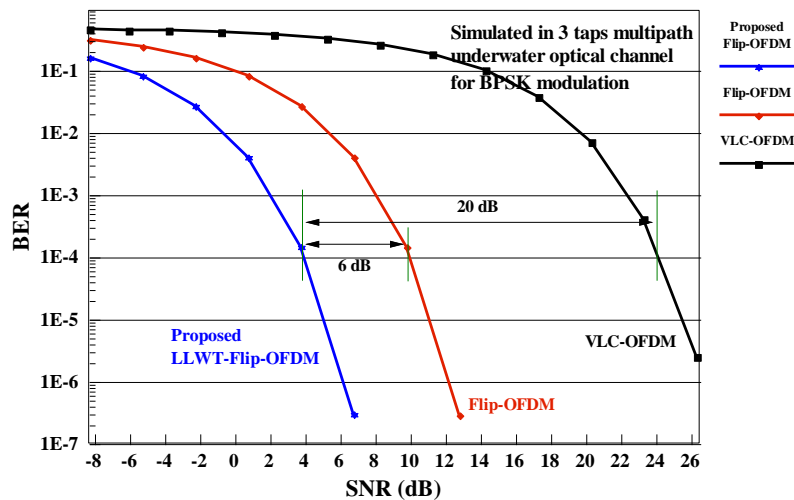


Fig. 19. Comparison of the proposed LLWT Flip-OFDM, VLC-OFDM and Flip-OFDM communication systems in three taps underwater OCIR for BPSK modulated signal (color online)

It is determined from Fig. 19 that the recommended LLWT Flip-OFDM communication system is approximately 6 dB better than the Flip-OFDM communication system and approximately 20 dB better than the VLC-OFDM communication system at $1E-3$ BER level for BPSK modulated signals.

5. Conclusion

In this article, LLWT Flip-OFDM waveform based on Lazy Lifting wavelet transform is proposed as an alternative to Flip-OFDM system from optical OFDM schemes. With the proposed waveform, computer simulation studies were carried out in both indoor multipath optical channel and underwater multipath optical channel environments. It has been seen from the results that the recommended LLWT Flip-OFDM communication system is 7.5 dB better than the Flip-OFDM communication system and 22.5 dB better than the VLC-OFDM communication scheme at the $1E-3$ BER level. Despite the increase in computational complexity, this increase in efficiency was significant. It has been revealed that the computational complexity taken into account in the realization of the proposed LLWT Flip-OFDM waveform will not create any problem with today's technology. As such, it is understood that the proposed waveform may be one of the best transmission systems for optical wireless telecommunication schemes that can be utilized for future beyond 6G implementations.

References

- [1] J. M. Kahn, J. R. Barry, Proceedings of the IEEE, **85**(2), 265 (1997).
- [2] Z. Xu, B. M. Sadler, IEEE Communications Magazine **46**(5), 67 (2008).
- [3] A. G. Bell, W. G. Adams, W. H. Tyndall, Journal of the Society of Telegraph Engineers **9**(34), 375 (1880).
- [4] D. K. Jackson, T. K. Buffaloe, S. B. Leeb, IEEE Transactions on Industry Applications **34**(3), 625 (1998).
- [5] VLCC, Visible light communication consortium, Accessed: September 2021, URL <http://www.vlcc.net/>.
- [6] Home gigabit access, omega, Accessed: September 2021, URL <http://www.ict-omega.eu/>.
- [7] C. Medina, M. Zambrano, K. Navarro, International Journal of Advances in Engineering & Technology **8**(4), 482 (2015).
- [8] Y. Tanaka, S. Haruyama, M. Nakagawa, IEEE 11th International Symposium on Personal, Indoor and Mobile Radio Communications (PIMRC 2000) **2**, 1325 (2000).
- [9] IEEE Standard for Local and Metropolitan Area Networks, Part 15.7: Short-Range Wireless Optical Communication Using Visible Light. IEEE Std 802.15.7-2011, **5**, 1-309 (2011).
- [10] R. D. Roberts, S. Rajagopal, S.-K. Lim, IEEE GLOBECOM Workshops **1**, 772 (2011).
- [11] S. Rajagopal, R. Roberts, S.-K. Lim, IEEE Communications Magazine, **50**(3), 72 (2012).
- [12] D. Karunatilaka, F. Zafar, V. Kalavally, R. Parthiban, IEEE Communications Surveys and Tutorials **17**(3), 1649 (2015).
- [13] S. Maheswari, Comparative study of various modulation schemes used in indoor VLC, MSc thesis, Indraprastha Institute of Information Technology, June, 2017, New Delhi.
- [14] J. Armstrong, Journal Lightwave Technology **27**(3), 189 (2009).
- [15] J. Kahn, J. Barry, Proceedings of the IEEE **85**(2), 265 (1997).
- [16] J. Armstrong, B. Schmidt, IEEE Communications

- Letters **12**(5), 343 (2008).
- [17] J. G. Proakis, M. Salehi, Digital Communications, 5th Edition, McGraw-Hill, 2008.
- [18] V. Kumbasar, O. Kucur, Wireless Telecommunication Symposium (WTS) **1**, 1 (2009).
- [19] E. Öksüz, A. Altun, A. Özen, IEEE 24th Signal Processing and Communications Applications SIU 2016, **1**, 1 (2016).
- [20] D. Karamehmedovic, M. K. Lakshmanan, H. Nikookar, Second International Workshop on Cognitive Radio and Advanced Spectrum Management (CogART) **1**, 45 (2009).
- [21] H. Sadreazami, M. Amini, Proceedings of fourth IET International Conference on Wireless, Mobile & Multimedia Networks (ICWMMN) **1**, 173 (2011).
- [22] M. Jansen, P. Ooninx, Second Generation Wavelets and Applications **1**, 21 (2005).
- [23] J. Maly, P. Rajmic, IFIP Int. Federation Inf. Process., Boston, MA, USA: Springer **245**, 488 (2007).
- [24] A. Güner, A. Özen, Journal of Lightwave Technology **39**(13), 4255 (2021).
- [25] Y. İ. Tek, E. B. Tuna, A. Savaşçıhabeş, A. Özen, International Journal of Electronics and Communications **138**(8), 1 (2021).
- [26] M. Maraş, E. N. Ayvaz, M. Gömeç, A. Savaşçıhabeş, A. Özen, Sensors **21**(5), 1 (2021).
- [27] P. Saengudomlert, 5th International Electrical Engineering Congress, Pattaya, Thailand **1**, 1 (2017).
- [28] S. Khalid, S. I. Shah, International Conference on Emerging Technologies (ICET) **1**, 179 (2006).
- [29] A. Güner, A. Özen, Optoelectron. Adv. Mat. **13**(9-10), 506 (2019).
- [30] W. Sweldens, SIAM J. Math. Anal. **29**(2), 511 (1998).
- [31] S. Temurtaş, Improving the Performance of Flip-OFDM Systems with Channel Encoders and Lifting Wavelet Transform for Visible Light Communications, Bachelor Degree Thesis, Nuh Naci Yazgan University – HARGEM, Kayseri, Turkey, June 2021.
- [32] F. Miramirkhani, M. Uysal, IEEE Photonics Journal **7**(6), 1 (2015).
- [33] F. Miramirkhani, M. Uysal, IEEE Access Journal **6**, 1082 (2018).

*Corresponding author: sinemtmrts98@gmail.com